1854

Cross-phase modulation effects in nonlinear fibre Bragg gratings

N. G. R.Broderick, D. Taverner, D. J. Richardson, M. Ibsen

Optoelectronics Research Centre, University of Southampton, Southampton, SO17 1BJ, UK.

Phone: +44 (0)1703 593144, Fax: +44 (0)1703 593142, email: ngb@orc.soton.ac.uk

May 13, 1999

Abstract

We report the results of a series of experiments examining cross-phase modulation effects in apodised fibre Bragg gratings. All-optical switching and the optical pushbroom are observed depending on the precise wavelength of the probe. The experimental results are then modelled using the coupled mode equations.

42.65.Pc,42.65.Re,42.70.Qs,42.81.-i

1. Introduction

Optical fibre Bragg gratings (FBG) possess many features which make them attractive to the telecommunication industry. Chief among these is the fact that they combine high reflectivity with a narrow bandwidth making them ideal for add/drop filters in a WDM system. These properties also offer the potential for the development of high quality nonlinear devices such as optical switches. The narrow bandwidth of a FBG means that only a small change in the refractive index is necessary to detune light from inside the bandgap (where the reflection is high) to outside it where complete transmission is possible. The strong reflectivity ensures that the contrast ratio between the off and on states of the grating is large. There are, of course, two ways to switch a Bragg grating. The first is to use an optical pulse, tuned to lie within the bandgap and whose intensity is sufficient to detune itself from resonance allowing propagation through the structure. Indeed recently we demonstrated a nonlinear increase in the transmission of a FBG from 2% to 40% using this method[1]. The second is to use a high intensity pump beam, tuned far from the Bragg resonance, to alter the propagation constant of a weak signal beam whose wavelength is near or within the grating bandgap. Such cross-phase modulation effects were first seen by LaRochelle *et al.*[2] and more recently ourselves[3,4].

Although the first approach is perhaps more aesthetically pleasing the second method offers considerable advantages for a practical device. Firstly, there is no restriction on the frequency separation between the pump and probe. This allows the pump and grating wavelengths to be chosen separately. Secondly, as there is no energy exchange between the pump and probe a single pump can switch multiple channels in a WDM system. Lastly there are no requirements on the probe intensity.

It is for these reasons that the first nonlinear experiments in FBGs used cross phase modulation (XPM) to switch a weak signal. LaRochelle *et al.* first demonstrated nonlinear switching in 1990[2] whereas the first reports of self-switching in a FBG did not appear till much later[1]. This time delay was due to the comparative ease of observing XPM effects over SPM effects in a FBG.

In the previous discussion we have not distinguished between CW and pulse effects however the differences are important and lead to very different behavior. In a Kerr medium the refractive index $n(x)$ can be modeled by

$$n(x) = n_0 + n^{(2)} I(x) \tag{1}$$

where n_0 is the background index and $I(x)$ is the local intensity. If we consider the effect of a strong CW pump beam on a low intensity signal then clearly the dominant effect is that the signal "sees" a constant refractive index which is slightly different from the background medium. The slight change in the effective refractive index however can still be sufficient to detune the signal from the Bragg grating (or any other resonant condition). If however the pump is a short intense pulse then via Eq. (1) it can be thought of as a moving wall of refractive index. The signal beam, upon encountering this moving wall, will be Doppler shifted and thus its frequency will be altered. More precisely it can be shown that the probe's frequency shift is proportional to the gradient of the pump's intensity profile[5]. In a medium with a positive Kerr nonlinearity ($n^{(2)} > 0$) a positive intensity gradient (e.g. the leading edge of the pump pulse) causes a red shift of the probe's frequency while a negative intensity gradient causes a blue shift of the probe's frequency. If the pulse is asymmetric then the frequencies shifts from the leading and trailing edges can be very different, as we show below. Also, as demonstrated later, the difference between CW and pulse effects leads to very different types of behaviour in Bragg gratings. Lastly we note that the effects we have been describing depend only on the intensity of the pump and not it's phase. If however the frequency difference between the pump and probe is sufficiently small then parametric amplification of the probe can take place[6]. For the purposes of this paper we restrict ourselves to the non-phase matched regime where any parametric amplification is negligible.

In this paper we present our experimental observations of the effects of cross phase modulation in FBGs. The outline of the paper is as follows, in Section 2 we present a theoretical model of our system, while in Section 3 we describe the experimental setup. In Section 4 and Section 5 we present our results along with a comparison of the results from our numerical model. Finally we discuss these results in Section 6.

2. Theoretical Model

In a fibre Bragg grating the linear refractive index varies periodically with a period d and can be approximated as[7]

$$n(z) = n_0 + \Delta n(z) cos(2k_0 z) \tag{2}$$

where n_0 is the background refractive index and $\Delta n(z)$ is the modulation depth of the grating. The wave-vector $k_0 = \pi/d$ and corresponds to the Bragg frequency ω_0 around which the grating is highly reflective. We take Eq. (2) to refer to the effective index of the fibre mode under consideration.

The effect of the grating is to couple forward and backward propagating light at frequencies ω close to ω_0. Thus in our model we can assume that there are only two frequencies of interest, the Bragg frequency ω_0 and the pump frequency ω_p. Also we assume that $|\omega_p - \omega_0|$ is sufficiently large so that the pump is unaffected by the grating, a condition satisfied in our experiments. Under these conditions we can write the electric field as

$$\mathbf{E}(z,t) = \left[f_+(z,t)e^{i(k_0 z-\omega_0 t)} + f_-(z,t)e^{-i(k_0 z+\omega_0 t)}\right]\hat{\mathbf{x}} + P(z,t)e^{i(k_p z-\omega_p t)}\hat{\mathbf{y}} + c.c. \tag{3}$$

where f_+, and f_+, are the slowly varying envelopes of the forward and backward propagating waves at the Bragg frequency. The pump envelope is given by $P(z,t)$ where z is the propagation direction. Note that we have taken the pump and probe to be orthogonally polarised which is not necessary but represents the experimental conditions. Making the usual slowly varying assumptions the coupled mode equations (CME) for f_+ and f_- can be written as[8]

$$i\frac{\partial f_+}{\partial x} + \frac{i}{v_g}\frac{\partial f_+}{\partial t} + \kappa f_- + \delta f_+ + \frac{2}{3}\Gamma|P(z,t)|^2 f_+ = 0, \tag{4a}$$

$$-i\frac{\partial f_-}{\partial x} + \frac{i}{v_g}\frac{\partial f_-}{\partial t} + \kappa f_+ + \delta f_- + \frac{2}{3}\Gamma|P(z,t)|^2 f_- = 0. \tag{4b}$$

Note that we have assumed that the pump propagates unchanged throughout the fibre, i.e. $P(z,t) = P(z - v_g t)$. For an optical fibre[7,9]:

$$\delta = \frac{\omega - \omega_0}{v_g}, \quad \kappa(z) = \frac{\pi \Delta n(z)}{\lambda}, \quad \Gamma = \frac{4\pi n_0}{\lambda Z} n^{(2)}, \tag{5}$$

v_g is the group velocity in the absence of a grating, λ is the free space Bragg wavelength and Z the vacuum impedance. The parameter κ measures the strength of the coupling between f_+ and f_-. In addition to Eq. (4) we assume that no light is incident upon the grating from the right, i.e backwards direction, and that initially the fields in the grating are in steady-state.

Eqs. (4) for the optical pushbroom are identical to those derived by de Sterke[8] except for two minor changes. Firstly, since we have an orthogonally polarised pump and probe the nonlinearity is reduced by a factor of three. Secondly, we have assumed a nonuniform grating so that κ is a function of position. In deriving Eq. (4) we have made two important assumptions. Firstly that the wavelength difference between the pump and probe is sufficiently large so that there is no parametric amplification of the probe beam. Secondly we have assumed that the probe beam is sufficiently weak so that by itself it does not experience any nonlinear effects. Both these effects have been included theoretically by others[10–12] but as such effects were not present in our experiments we do not include them in our model.

A. Linear Properties of a Fibre Bragg grating

To understand the nonlinear behavior of a FBG first recall the linear properties. In the absence of a pump and for a CW input the coupled-mode equations can be written as

$$\frac{\partial}{\partial x}\begin{pmatrix} f_+(x) \\ f_-(x) \end{pmatrix} = \begin{pmatrix} i\delta & i\kappa(x) \\ -i\kappa(x) & -i\delta \end{pmatrix}\begin{pmatrix} f_+(x) \\ f_-(x) \end{pmatrix} \tag{6}$$

For a uniform grating ($\kappa(x) = \kappa$) we can solve Eqs. (6) by exponentiating, yielding the transfer matrix M:

$$M = \frac{1}{\beta}\begin{pmatrix} i\delta \sin\beta x + \beta\cos\beta x & i\kappa\sin\beta x \\ -i\kappa\sin\beta x & \beta\cos\beta x - i\delta\sin\beta x \end{pmatrix} \tag{7}$$

where $\beta^2 = \delta^2 - \kappa^2$. Eq. (7) is still valid when β is complex, which occurs when $|\delta| < \kappa$. In terms of M the solutions to the coupled mode equations are:

$$\begin{pmatrix} f_+(x) \\ f_-(x) \end{pmatrix} = M\begin{pmatrix} f_+(0) \\ f_-(0) \end{pmatrix} \tag{8}$$

From Eq. (8) it can easily be shown that for a finite structure the reflection coefficient is given by $r = -M_{11}/M_{21}$ and that there are discrete frequencies where the reflectivity drops to zero[13]. These zeros are important for the discussion of the optical pushbroom in Sect. 2 C.

For a uniform grating the bandgap extends from $-\kappa < \delta < \kappa$ and for frequencies within this region the intensity decreases exponentially along the length of the grating. Outside this region there are plane wave solutions to Eq. (6) which propagate unchanged through the grating and these can be written as

$$\begin{pmatrix} f_+ \\ f_- \end{pmatrix} = \begin{pmatrix} \kappa \\ q \mp \sqrt{q^2+\kappa^2} \end{pmatrix} e^{i(qx-\delta t)}, \tag{9}$$

where

$$q = \pm\sqrt{\delta^2 - \kappa^2}. \tag{10}$$

The dispersion relationship given by Eq. (10) is illustrated in Fig. 1. The group velocity V is

$$V = \frac{d\delta}{dq} = \frac{1}{\delta}\sqrt{\delta^2 - \kappa^2}. \tag{11}$$

Note that $V = 0$ at the band edge and asymptotically approaches unity as $\delta \to \infty$ indicating that the dispersion relationship approaches that of the background medium far from the grating, as one would expect. In addition the group velocity dispersion is given by the curvature of the dispersion relationship. From Fig. 1 it can be seen that this is anomalous above the bandgap and normal below it. For typical grating parameters the dispersion near the bandgap can be 6 orders of magnitude greater than the bare fibre dispersion which is why we have treated the background material as dispersionless in Eq. (4).

B. CW switching of a Fibre Bragg grating

By far the simplest application of the CMEs (Eqs. (4)) is the modelling of the switching of a uniform grating by a strong CW pump beam. In this case both κ and P are constants and the CMEs can then be solved exactly. The only effect the pump has on the solution is to introduce an additional detuning of $2/3\Gamma|P|^2$. This has the effect of uniformly shifting the entire reflection spectrum to lower detunings by $2/3\Gamma|P|^2$. For a uniform grating the frequency difference between the centre of the bandgap and the position of the first minima in the reflection spectrum is $\approx \kappa$. Thus the intensity needed to switch a probe, centred at the Bragg frequency from being reflected to being totally transmitted is[2]

$$|P|^2 \approx \frac{3}{2\Gamma}\kappa. \tag{12}$$

This effect was first seen by LaRochelle *et al.*[2] who observed an increase in the average power transmission from 4% to 6%. The degree of switching they were able to observe was limited by the temporal resolution of their detector and theoretical estimates suggest that actually complete switching was occuring in their system[2]. In LaRochelle's experiments the pump beam was in fact a 100 ps long pulse. However as their grating was only 3.5cm long the pulse was longer than the grating, justifying the CW nature of the experiment. We shall return to the question of what constitutes a CW pump later in the paper.

For our experiments we have used a nonuniform grating. In the CW regime this makes no differences to the physics, however the switching power may be increased or decreased depending on whether the bandgap is larger or smaller than that of a uniform grating (i.e. κ in Eq. (12) should be replaced by κ_{max}).

C. The Optical Pushbroom

In the regime that the pump pulse is shorter than the grating then the interaction can no longer be treated as though it were CW. In this regime the dominant effect is the frequency shift of the probe rather than the nonlinearly induced shift in the Bragg resonance. This frequency shift can result in the compression of the probe – the so called optical pushbroom[8]. This works as follows.

From Eq. (11) it can be seen that the further away a pulse is from the bandgap the greater its group velocity. Clearly then a FBG could be used to efficiently compress an appropriately chirped pulse as it propagates through the grating. The basics of the optical pushbroom are that the intense pump introduces a chirp on the probe pulse which is then compressed by the FBG. More precisely consider a CW beam centred at the first transmission resonance of the FBG. The intensity profile of the light inside the grating is shown in Fig. 2. Note that a significant amount of energy is stored inside the grating at this detuning. When the pump enters the grating it first encounters the back of the probe resonance. Through XPM it lowers the frequency of the back of the probe causing it to speed up. This increase in velocity allows the back of the probe to sit on the leading edge of the pump where it experiences still further XPM. This process continues through the grating with more and more of the probe's energy being swept up onto the leading edge of the pump.

In transmission the hallmark of the optical pushbroom is thus a sharp spike (temporally coincident with the pump) followed by a relatively longer dip in the transmission. The decrease in transmission is due to the fact that the pump has swept up all the stored energy in the grating and the transmission resonance needs time to re-establish itself. The effects of the optical pushbroom can be seen in Fig. 3 which shows a theoretical trace of the transmitted light obtained by solving Eq. (4) numerically. In the simulation the various parameters were chosen to correspond to the measured experimental values.

In its original guise the optical pushbroom was shown to work in a uniform Bragg grating where it swept out the energy associated with one of the linear resonances[8]. The same physical process was soon shown to compress optical pulses which were co-propagating with the pump through the grating[6,14]. However as Fig. 3 shows the same effect can be seen in apodised gratings which do not have as strong resonances as uniform Bragg gratings. The optical pushbroom works in this case since for frequencies close to the edge of the bandgap there is still an appreciable amount of energy stored in the grating which can be swept out via cross-phase modulation (see Fig. 2). In fact the use of an apodised grating considerably relaxes the experimental requirements to see the optical pushbroom. Because of the lack of any well-defined resonances in the transmission spectrum the detuning of the probe does not need to be as critically tuned as it would if the probe had to lie exactly on a transmission resonance. Thus as we show below for an apodised grating there are a wide range of frequencies where the optical pushbroom can be observed.

The wide range of possible behaviours that can be observed in a nonuniform Bragg gratings are shown in Fig. 4 and Fig. 5. These graphs show the transmitted (dashed lines) and reflected intensities (solid lines) for a CW beam at various detunings. The parameters used in these simulations match as closely as possible the experimental parameters described below. In Fig. 4 the detuning is above the centre of the bandgap and simple CW switching can be seen particularly in Fig. 4(b) and (c). In Fig. 5 the detuning is below the centre of the bandgap and as expected optical push broom effects can be seen. Note that due to the length of the pump pulse we can assume that the field in the grating evolves adiabatically (except for the first 100ps due to the sharp leading edge of the pump) and thus at most times the reflection and transmission should sum to unity as can be seen in the theoretical traces.

3. Experimental Setup

Our experimental setup is shown in Fig. 6. High power pump pulses at 1550nm are used to switch a low-power (1mW) , narrow-linewidth ($<$ 10 MHz) probe that could be temperature tuned right across the grating's bandgap. The pump pulses, derived from a directly modulated DFB laser, were amplified to a high power ($>$ 10 kW) in an erbium doped fibre amplifier cascade based on large mode area erbium doped fiber and had a repetition frequency of 4KHz. Fig. 8 shows the intensity profile of the pump pulse. It's shape is asymmetric due to gain saturation effects within the amplifier chain and has a 30ps rise time and a 3ns half-width. The spectral half-width of the pulses at the grating input was measured to be 1.2 GHz, as defined by the chirp on the input seed pulses.

The pump and probe were polarization coupled into the FBG and were thus orthogonally polarised within the FBG. A half-wave plate was included within the system allowing us to orient the beam along the grating birefringence axes. Both the reflected and transmitted probe signals could be measured in our experimental system using a fiberized detection system based on a tunable, narrow-band ($<$ 1nm) optical filter with $>$80 dB differential loss between pump and probe (sufficient to extinguish the high intensity pump signal), a low noise pre-amplifier, a fast optical detector and sampling scope. The temporal resolution of our probe beam measurements was $\approx$50ps.

The FBG was centered at 1536 nm and was 8 cm long with an apodised profile resulting in almost complete suppression of the side-lobes. The grating had a peak reflectivity of 98% and a measured width of less than 4 GHz. The measured reflection spectrum is shown in Fig. 7 (solid line), along with a theoretical reflection spectrum for an idealised grating with identical parameters. In Fig. 7 the wavelengths along the X-axis are given in terms of the difference from the centre wavelength of 1535.930 nm. The grating was mounted in a section of capillary tube, angle polished at both ends so as to eliminate reflections from the grating end faces and was appropriately coated to strip cladding modes.

It should be noted that the pump pulse shape requirements for CW switching and the optical pushbroom are somewhat incompatible. The pushbroom requires pulses with a large intensity gradient while to see CW effects the intensity gradient should be zero. However with our pulse we are able to have our cake and eat it too. The exceedingly rapid rise time of pulse allows us to see the optical pushbroom yet the fact that the pulse is longer than the grating allows CW effects to be seen. As we discuss in detail below the frequency of the probe pulse determines whether we are in a pushbroom or CW regime. In some cases however we see a combination of both effects.

We were able to tune the wavelength of our probe beam by changing the temperature of the laser diode. The following empirical relationship was found between the wavelength and the resistance of the heating element

$$\lambda(T) = 1538.00 - 0.149639T - 0.00199972T^2 \tag{13}$$

where T is measured in kΩ and λ in nanometres. We were able to control the temperature to within 0.01 kΩ corresponding to a wavelength tuneability of 1pm. The actual centre wavelength of the grating was constantly shifting due to small temperature changes of the laboratory making it hard to determine the actual detuning of the probe from the Bragg wavelength. In this paper we estimated the detuning by measuring the amount of reflected or transmitted light and comparing it to that measured at large detunings (where the transmission is assumed to be unity).

We performed a series of measurements looking at both the transmitted and reflected light as a function of both the probe wavelength and the pump power. These results are split into the reflected and transmitted outputs for clarity. We will first discuss the transmitted light case.

4. Forward Propagating Case

As discussed in Section. 2 the transmitted probe shape is expected to be a strong function of its detuning from the gratings bandgap. This can be seen in Fig. 9 and Fig. 10 which show the averaged probe's waveform as we tune across the bandgap from the short wavelength side to the long wavelength side while keeping the pump power constant. In these graphs the transmitted intensity has been scaled so that the normalised linear intensity at the centre of the bandgap is 0.04 while the normalised intensity at wavelengths well outside the bandgap is unity. This in fact slightly underestimates the true transmission for long wavelengths due to a slight wavelength dependence of the detection process. In all the traces the origin of the time is set to coincide with the start of the transmitted pump pulse. These experimental traces should be compared to the theoretical traces in Fig. 4.

Examining the traces in Fig. 9 we see that the common feature is that the transmission increases in the presence of the pump. This is due to the nonlinear index change induced by the pump which shifts the Bragg wavelength to lower frequencies and thus the probe is effectively further from the Bragg resonance, hence it's transmission increases. In this regime our results are similar to those of La Rochelle et al.[2]. The most important difference being that we are able to resolve the temporal shape of the transmitted light. In addition we have a cleaner source and a better grating giving significantly clearer results. Note that in cases (a) and (b) the transmission follows very closely the pump profile in Fig. 8 due to the fact that the grating's slope is almost linear near the short wavelength edge. However as we move closer towards the centre of the Bragg grating only the peak of the pulse is sufficiently intense to switch the probe. Hence instead of seeing the broad switched pulses there is only a narrow pulse corresponding in time to the peak of the pump pulse. This can also be clearly seen in Fig. 4(d).

In Fig. 10 the traces for frequencies below the bandgap are shown where again we see a strong dependence on the probe's wavelength. As we are now below the Bragg resonance the effect of the pump is to move the probe's wavelength closer to the centre of the bandgap thereby decreasing the transmission. This is the cause of the long dips in the transmission which can be seen in all the traces. In addition to the dips in the transmission it can also be seen that the transmission initially increases due to the presence of the pump. This is the optical pushbroom effect described above. As expected it can only be seen for frequencies close to the long wavelength edge of the grating. However, as discussed in Section 2 C, this wavelength range is much broader than that of a comparable uniform grating. Again these features can be seen in the theoretical traces. However in the theoretical case the degree of switching is typically larger than that seen in the experiments. This is due largely to the difference in pulse shapes between the theory and experiments. The theoretical pulse shape decays more smoothly than the experimental one. However note that the overall agreement is excellent with small features such as the increase in the transmitted light at $t = 3$ns in Fig. 10(e) also appearing in the corresponding theoretical trace [Fig. 5(e)].

Optimising the wavelength for the optical pushbroom results in the trace shown in Fig. 11a. In this case the probe was detuned by 0.02nm from the Bragg resonance which is right on the very edge of the grating resonance where the transmission is near unity in the absence of the probe. Note that the parameters used in the theoretical trace (Fig. 3) correspond as closely as possible to the experimental parameters of Fig. 11a. Note that there is an excellent agreement between the theoretical and experimental trace which is matched by the agreement at other detunings. This allows us to be confident that we are observing the optical pushbroom and not some other nonlinear effect. One again the main disagreement between the two comes from the difference in pulse shapes between the theoretical model which assumed a triangular pulse and the actual pump profile which is more complicated (see Fig. 8).

Lastly we examined the effects of changing the pump power on the transmitted profiles. These results are shown in Fig. 11b and basically followed the expected trend. Since we are examining a nonlinear effect it should die away with decreasing pump power as indeed it does. We now turn to the traces of the reflected light which have not been treated before either analytically or experimentally in any detail.

5. Backward Propagating Case

In Fig. 12 and Fig. 13 are shown the reflected traces of the probe as a function of time. These traces are normalised so that the peak reflection in the linear regime corresponds to a value of 0.96. This normalisation again underestimates slightly the actual reflectivity for frequencies near the edge of the bandgap due to the uneven gain from the amplifier before the detector. We not that due to a thermal shift in the Bragg resonance of the grating the actual detunings in Fig. 12 and Fig. 13 are different to those in Fig. 9 and Fig. 10 even though the actual temperature of the diode was the same in each case.

Looking at the traces in Fig. 12 and Fig. 13 a number of features are apparent. Firstly as expected the reflectivity decreases in the presence of the pump above the bandgap and increases below the bandgap. This is due to the simple effect of cross-phase modulation as discussed in Section. 4 whereby the effective frequency of the centre of bandgap decreases due to the presence of the pump. Compared however to the transmitted cases the effects of cross-phase modulation are not as apparent [e.g. compare Fig. 9(b) with Fig. 12(b)]. We are not fully confident of the reason for this but it is most likely due to a drop in the pump power during the course of the measurements.

The other main feature of interest in the reflected traces can be seen in Fig. 12(a). Note that initially the reflected intensity increases in a manner similar to the traces of the optical pushbroom. This is a new effect caused by the apodisation profile of the grating and which could not have been seen if one used a uniform grating[4]. Note that this can also be clearly in Fig. 4(a). The reason behind this peak is very similar to the explanation for the optical pushbroom in that a nonlinear shift in frequency is responsible for the appearance of the peak. In our situation, due to the apodisation profile light propagates through almost half the grating before being reflected. This means that compared to a uniform grating significantly more energy is stored in the grating at frequencies within its bandgap. The pump pulse acts on this stored energy by lowering its frequency through cross phase modulation. The apodisation profile then ensures that lower frequencies are reflected earlier in the grating and thus creates the right amount of dispersion to compress the reflected pulse.

Unlike the forward pushbroom this effect can only be seen in apodised gratings and it takes place over a narrower frequency range as can be seen from the experimental traces. We have performed numerical simulations which show that it is a robust phenomenon which occurs in a wide variety of nonuniform gratings including linearly chirped gratings. It is also possible to increase the size of the effect by appropriately designing the grating however it will always remain a relatively small effect compared to the optical pushbroom as less energy is stored in the grating at frequencies within the bandgap compared to frequencies outside the bandgap.

6. Conclusion

We have presented for the first time to our knowledge a complete investigation of the effects of cross-phase modulation showing the effects of varying the pump power and probe frequency on both the reflected and transmitted light. These experimental results can be accurately modelled using the standard coupled mode equations indicating that no other effects are present in our experiments.

The results here clearly show how a number of different pheomena such as the optical pushbroom and CW-switching of gratings which were previously considered separately, need to be considered together to obtain a complete understanding of our measurements. In addition these results show the advantage of using apodised gratings for such experiments. Apodised gratings are important since they allow light to penetrate further into the grating at frequencies within the bandgap in the linear regime making it easier to observe nonlinear effects[15]. Using apodised gratings allows for novel effects to be seen which were not previously predicted due to the theoretical focus on pulse dynamics in uniform gratings. These effects clearly show that it is possible to obtain significant switching using all-fiberised sources and gratings. Finally the agreement between the theoretical modelling and the experimental results gives us faith in our numerical model and should allow for the development of improved and functional devices based on fibre Bragg gratings.

REFERENCES

1. D. Taverner, N. G. R. Broderick, D. J. Richardson, M. Isben, and R. I. Laming, "Nonlinear Self-Switching and Multiple Gap Soliton Formation in a Fibre Bragg Grating," Opt. Lett. **23,** 328–330 (1998).

2. S. LaRochelle, Y. Hibino, V. Mizrahi, and G. I. Stegeman, "All-Optical Switching of Grating Transmission using Cross-Phase Modulation in optical fibres," Elect. Lett. **26,** 1459–1460 (1990).

3. N. G. R. Broderick, D. Taverner, D. J. Richardson, M. Isben, and R. I. Laming, "Optical pulse compression in fibre Bragg gratings," Phys. Rev. Lett. **79,** 4566 (1997).

4. N. G. R. Broderick, D. Taverner, D. J. Richardson, M. Isben, and R. I. Laming, "Experimental Observation of nonlinear pulse compression in nonuniform Bragg gratings," Opt. Lett. **22,** 1837–1839 (1997).

5. G. P. Agrawal, *Nonlinear Fibre Optics* (Academic Press, San Diego, 1989).

6. M. J. Steel and C. M. de Sterke, "Schrödinger equation description for cross-phase modulation in grating structures," Physics Review A **49,** 5048–5055 (1994).

7. J. E. Sipe, L. Poladian, and C. M. de Sterke, "Propagation through nonuniform grating structures," J. Opt. Soc. Am A **11,** 1307–1320 (1994).

8. C. M. de Sterke, "Optical push broom," Optics Letters **17,** 914–916 (1992).

9. C. M. de Sterke and J. E. Sipe, "Coupled modes and the nonlinear Schrödinger equation," Phys. Rev. A **42,** 550–555 (1990).

10. M. J. Steel and C. M. de Sterke, "Continuous-wave parametric amplification in Bragg gratings," JOSA B **12,** 2445–2452 (1995).

11. M. J. Steel and C. M. de Sterke, "Parametric amplification of short pulses in optical fiber Bragg gratings," Phys. Rev. E **54,** 4271–4284 (1996).

12. N. G. R. Broderick, "Bistable switching in nonlinear Bragg gratings," Opt. Comm. **148,** 90–94 (1998).

13. N. Broderick and C. M. de Sterke, "Analysis of Nonuniform Gratings," Phys. Rev. E **52,** 4458–4464 (1995).

14. M. J. Steel, D. G. A. Jackson, and C. M. de Sterke, "Approximate model for optical pulse compression by cross- phase modulation in Bragg gratings.," Physics Review A **50,** 3447–3452 (1994).

15. D. Taverner, N. G. R. Broderick, D. J. Richardson, R. I. Laming, and M. Isben, "Nonlinear self-switching and multiple gap-soliton formation in a fiber Bragg grating," Opt. Lett. **23,** 328–330 (1998).

FIGURES

Fig. 1. Dispersion relationship for a uniform grating with the same parameters as the one in Fig. 7. Note that no solutions exist in the bandgap. The dashed lines indicate the background dispersion relationship.

Fig. 2. Field profile inside the grating at the first transmission resonance. The solid line gives the total intensity $|f_+|^2 + |f_-|^2$ while the short dashed line indicates $|f_+|^2$ and the long dashed line gives $|f_-|^2$. Note that the field structure is single peaked with the maximum intensity being significantly higher than the input intensity illustrating the energy storage capability of a FBG.

Fig. 3. Theoretical trace of the optical pushbroom. The solid line is the transmitted probe intensity, while the dashed line shows the pump profile. The insert is a blowup of the front spike in the transmission. The parameters chosen match those used in the actual experiment.

Fig. 4. Theoretical transmitted (dashed lines) and reflected (solid line) intensity profiles of the probe beam as a function of the time in nanoseconds. The pump is incident upon the grating at $t = 0$. The detunings used were 0.662 cm^{-1}, 0.466 cm^{-1}, 0.049 cm^{-1} and -0.197 cm^{-1} for figures (a), (b), (c) and (d) respectively.

Fig. 5. Theoretical transmitted (dashed lines) and reflected (solid line) intensity profiles of the probe beam as a function of the time in nanoseconds. The pump is incident upon the grating at $t = 0$. The detunings used were -0.444 cm^{-1}, -0.592 cm^{-1}, -0.643 cm^{-1} and -0.891 cm^{-1} for figures (e), (f), (g) and (h) respectively.

Fig. 6. Schematic of the experimental setup. PBS: polarization beam splitter. BPF: bandpass filter with a width of < 1 nm. LA-EDFA: Large mode area Erbium fibre amplifier. The polarizer (POL) is set to minimize the pump. See the text for more details.

Fig. 7. Measured reflection spectrum of the grating used in our experiments (solid line). The dashed line is a theoretical trace for a grating with the same parameters. The centre of the grating is at 1535.9290nm and the horizontal scale gives the wavelength difference from the centre wavelength. The effect of the apodisation can be clearly seen in the lack of sidelobes in the spectrum.

Fig. 8. Measured intensity profile of the pump pulse used in the experiments.

Fig. 9. Measured transmitted intensity profiles of the probe pulses as a function of the time in nanoseconds. The derived detunings are 0.662 cm^{-1}, 0.466 cm^{-1}, 0.049 cm^{-1} and -0.197 cm^{-1} for figures (a), (b), (c), (d) respectively. In these traces the probe's intensity has been normalised to the peak of the transmission at wavelengths far from the grating.

Fig. 10. More transmitted intensity profiles for frequencies below the centre of the bandgap. The derived detunings are -0.444 cm^{-1}, -0.592 cm^{-1}, -0.643 cm^{-1} and -0.891 cm^{-1} for figures (e),(f),(g),(h) respectively.

Fig. 11. Experimental traces of the optical pushbroom. On the left shows the result of optimising the wavelength for maximum energy storage in the Bragg grating. The figure on the right shows the effect on increasing the pump power.

Fig. 12. Measured reflected intensity profiles of the probe pulses as a function of the time in nanoseconds (horizontal axis). The detuning of the probe is 0.588 cm^{-1}, 0.490 cm^{-1}, 0.246 cm^{-1} and 0.000 cm^{-1} for traces (a), (b), (c) and (d) respectively. In these traces the probe's intensity has been normalised so that the peak reflection in the linear regime corresponds to a value of 0.96.

Fig. 13. More reflected intensity profiles for frequencies below the centre of the bandgap. The detuning of the probe is -0.247 cm^{-1}, -0.494 cm^{-1}, -0.593 cm^{-1} and -0.643 cm^{-1} for traces (e), (f), (g) and (h) respectively. The graphs are normalised as in Fig. 13.

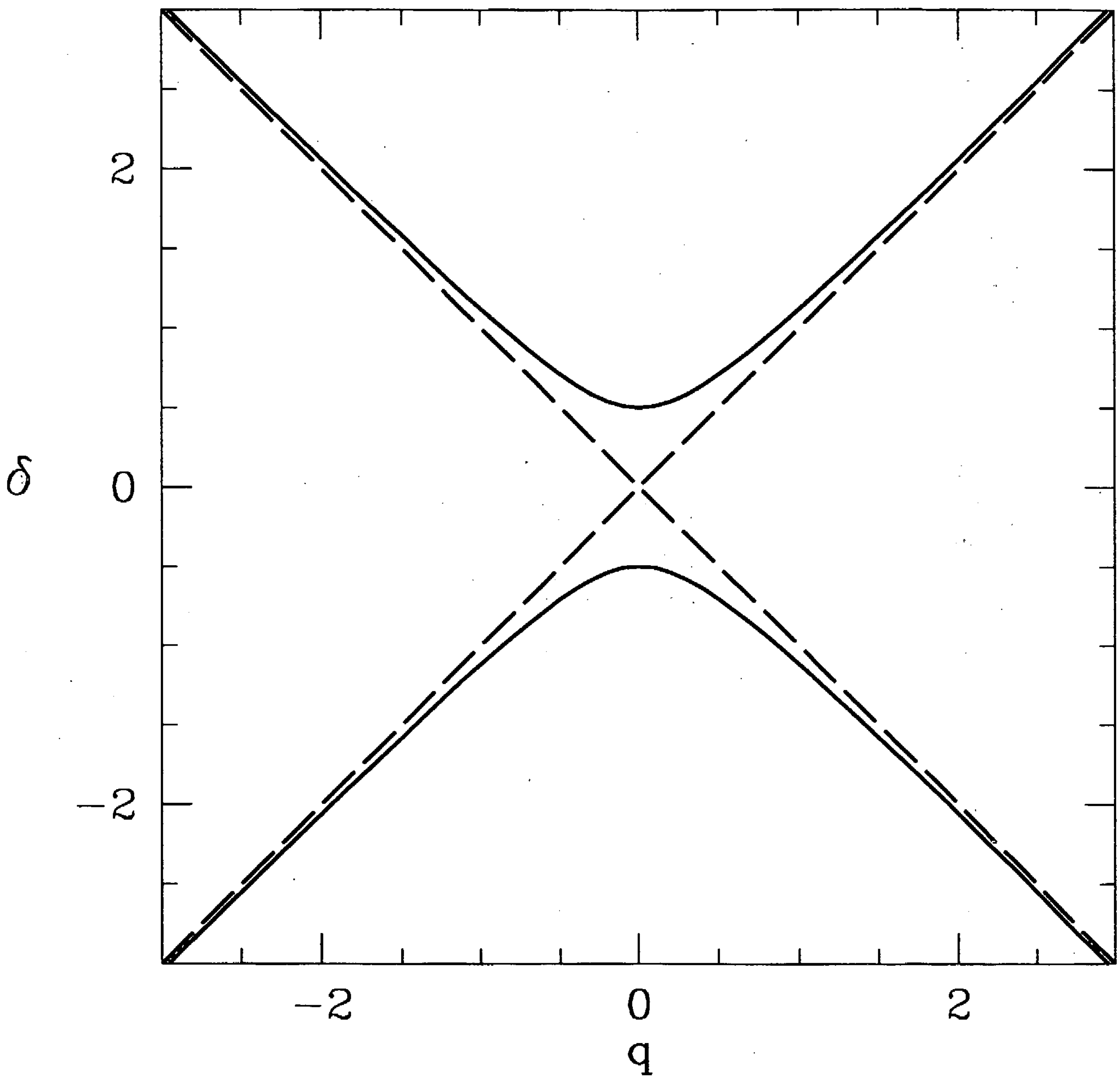

2
0
−2
δ
−2
0
2
q

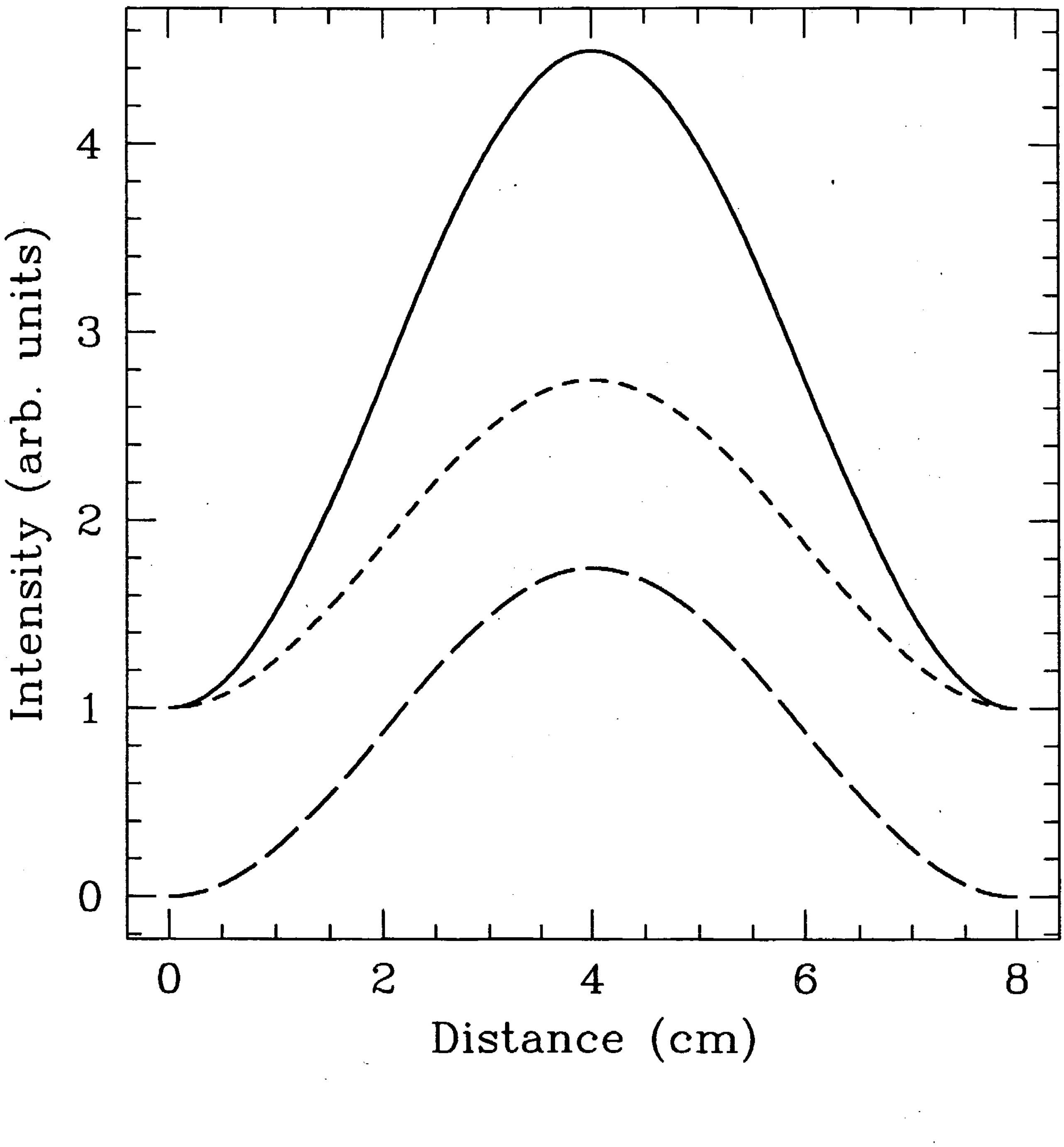

Intensity (arb. units)
0
1
2
3
4
0
2
4
6
8
Distance (cm)

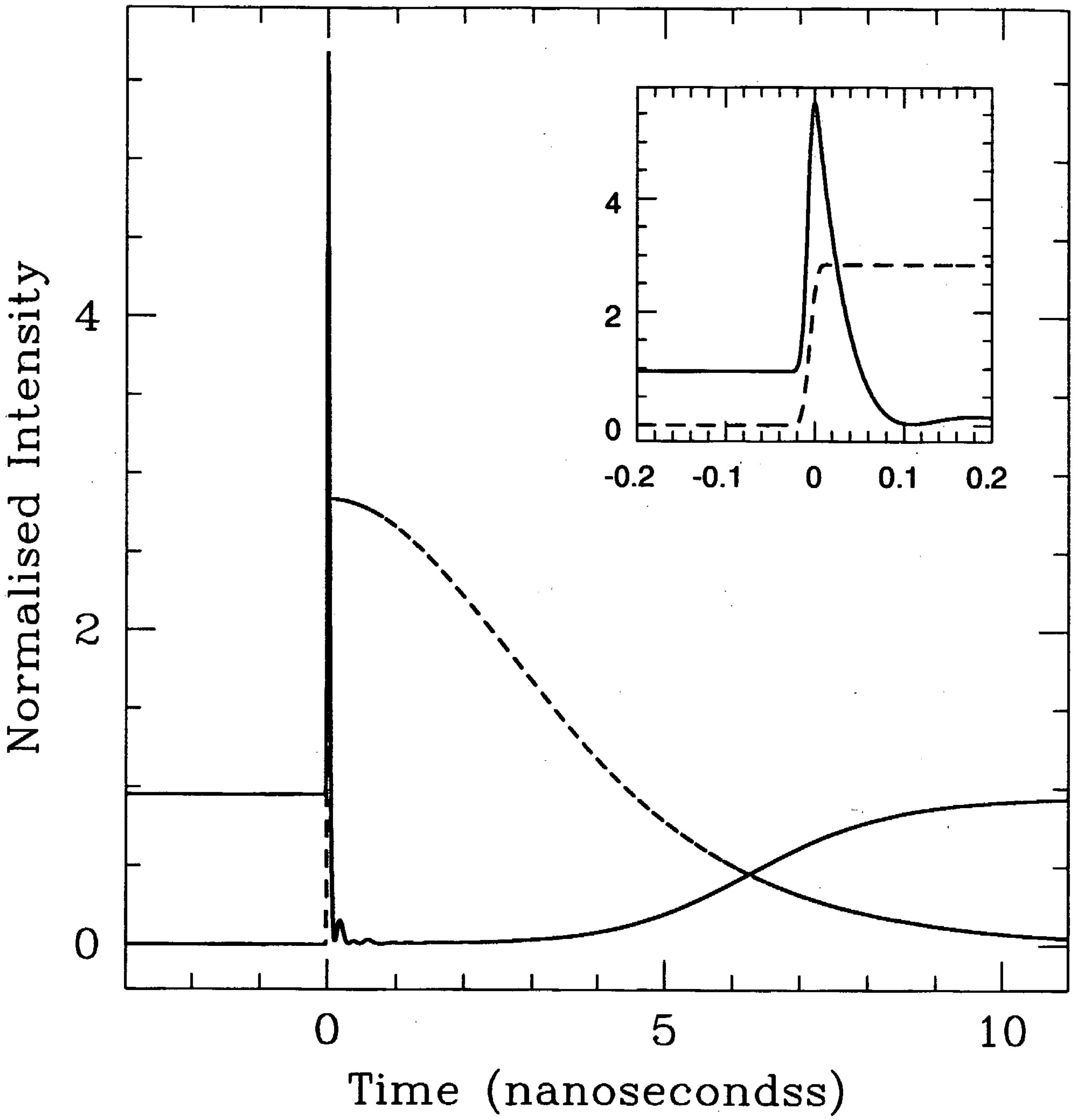
Normalised Intensity
Time (nanosecondss)
0
5
10
0
2
4
-0.2
-0.1
0
0.1
0.2
0
2
4

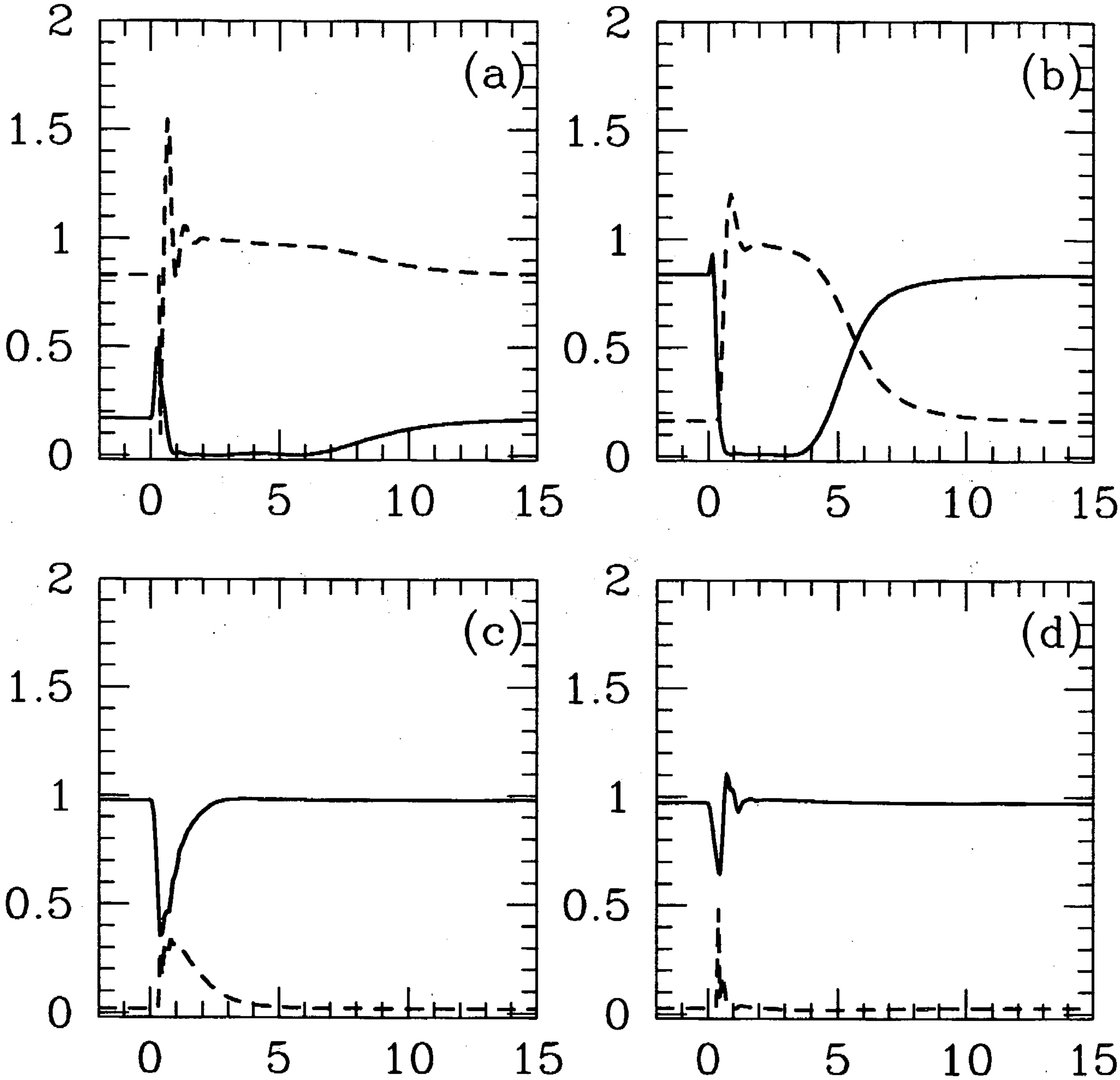

(a)
(b)
(c)
(d)
2
1.5
1
0.5
0
0
5
10
15

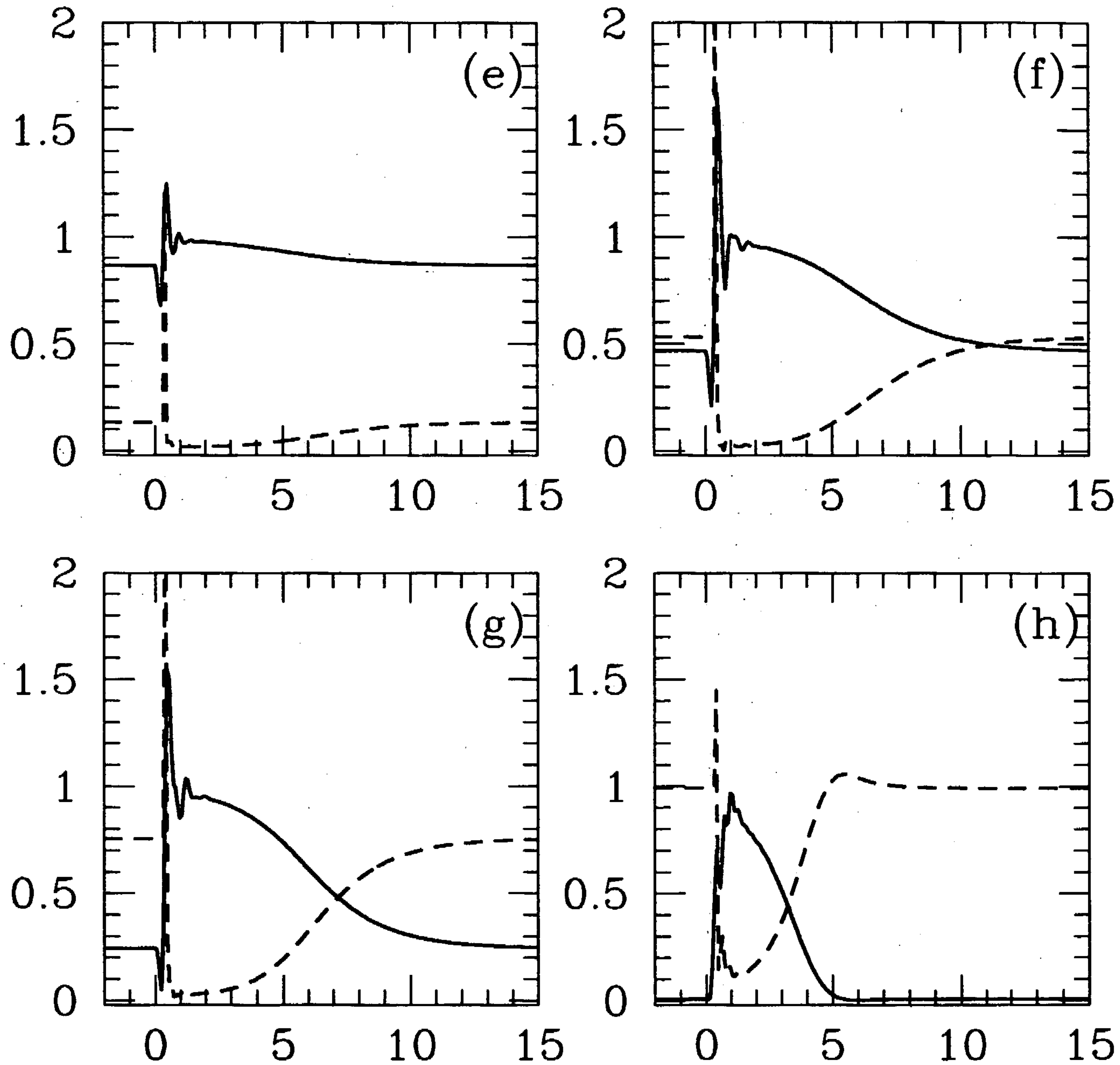

(e)
(f)
(g)
(h)
2
1.5
1
0.5
0
0
5
10
15

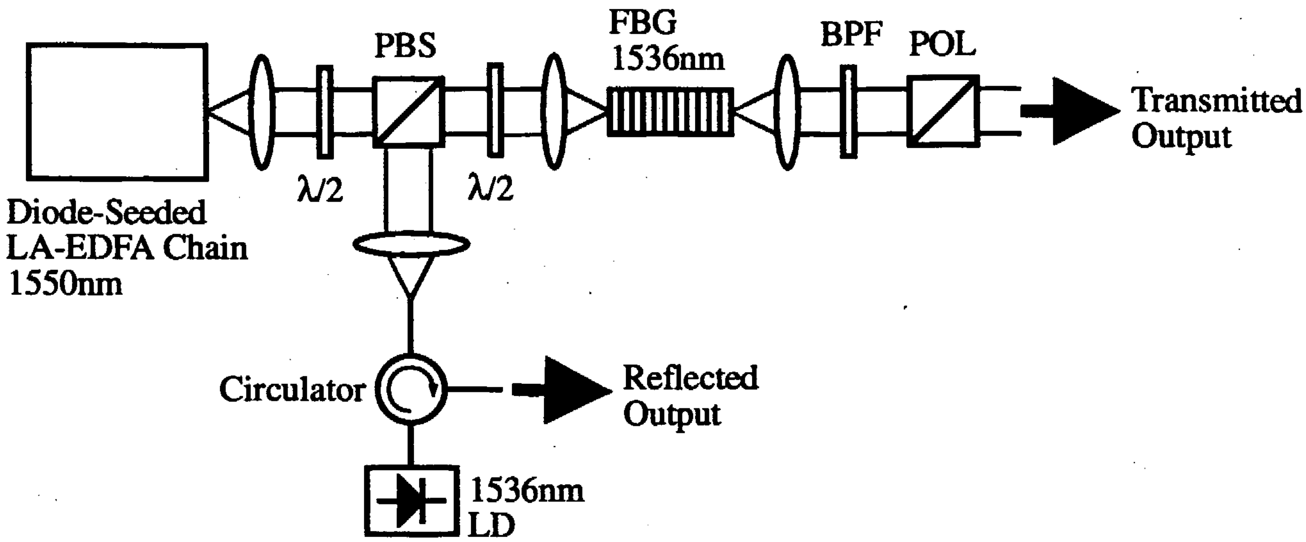

PBS
FBG
1536nm
BPF
POL
Transmitted
Output
Diode-Seeded
LA-EDFA Chain
1550nm
λ/2
λ/2
Circulator
Reflected
Output
1536nm
LD

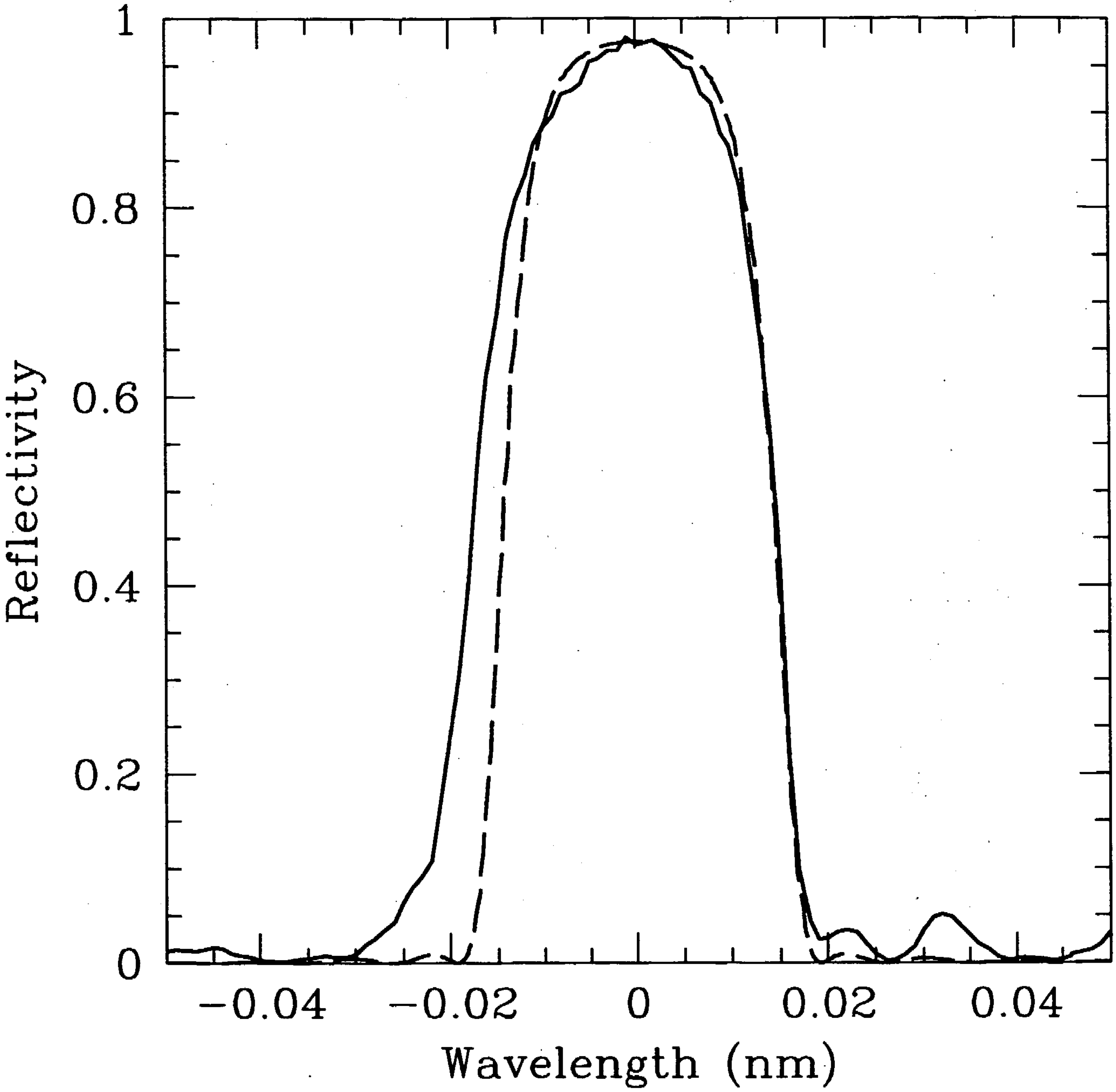

1
0.8
0.6
0.4
0.2
0
Reflectivity
−0.04
−0.02
0
0.02
0.04
Wavelength (nm)

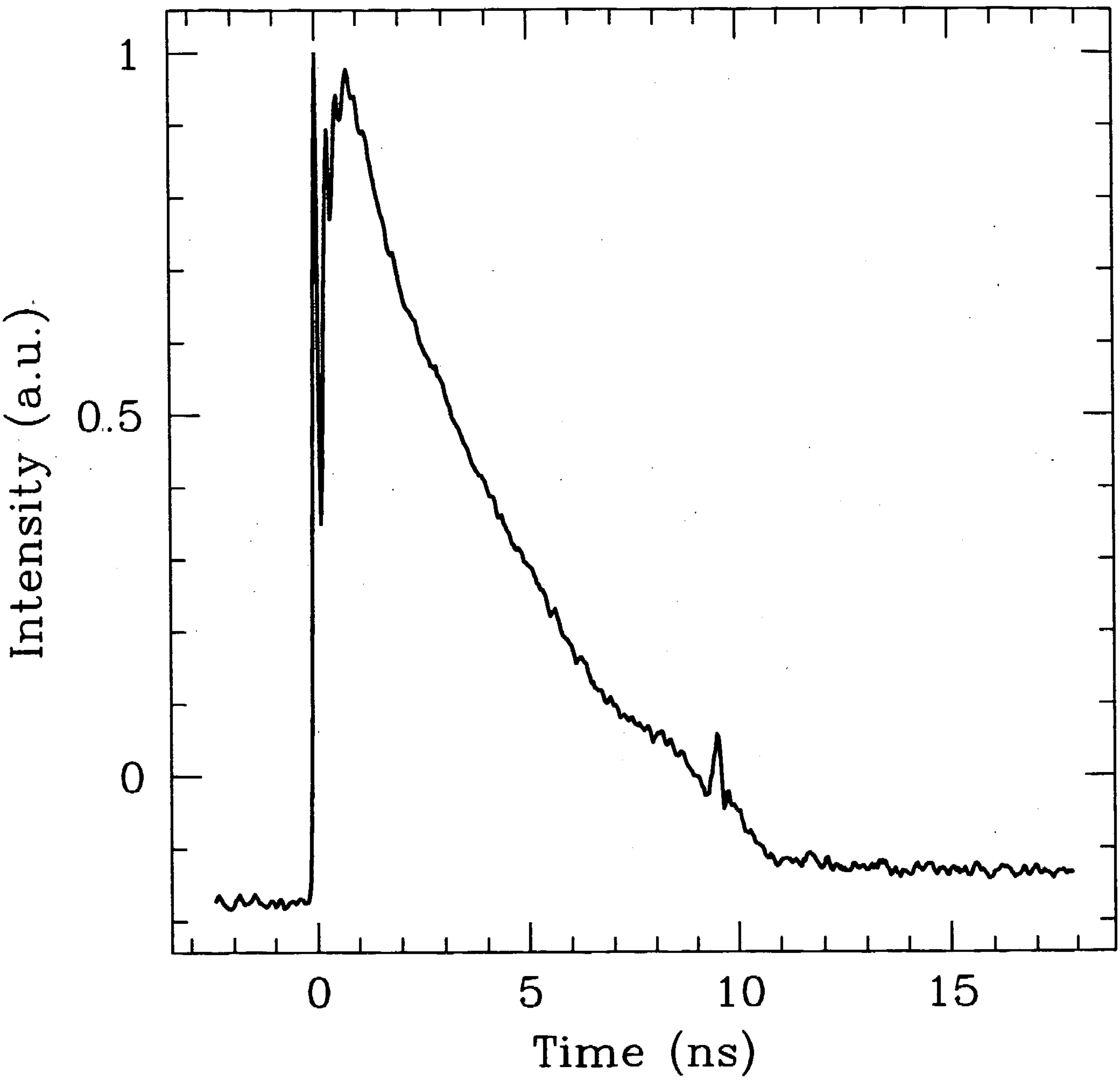

1
0.5
0
Intensity (a.u.)
0
5
10
15
Time (ns)

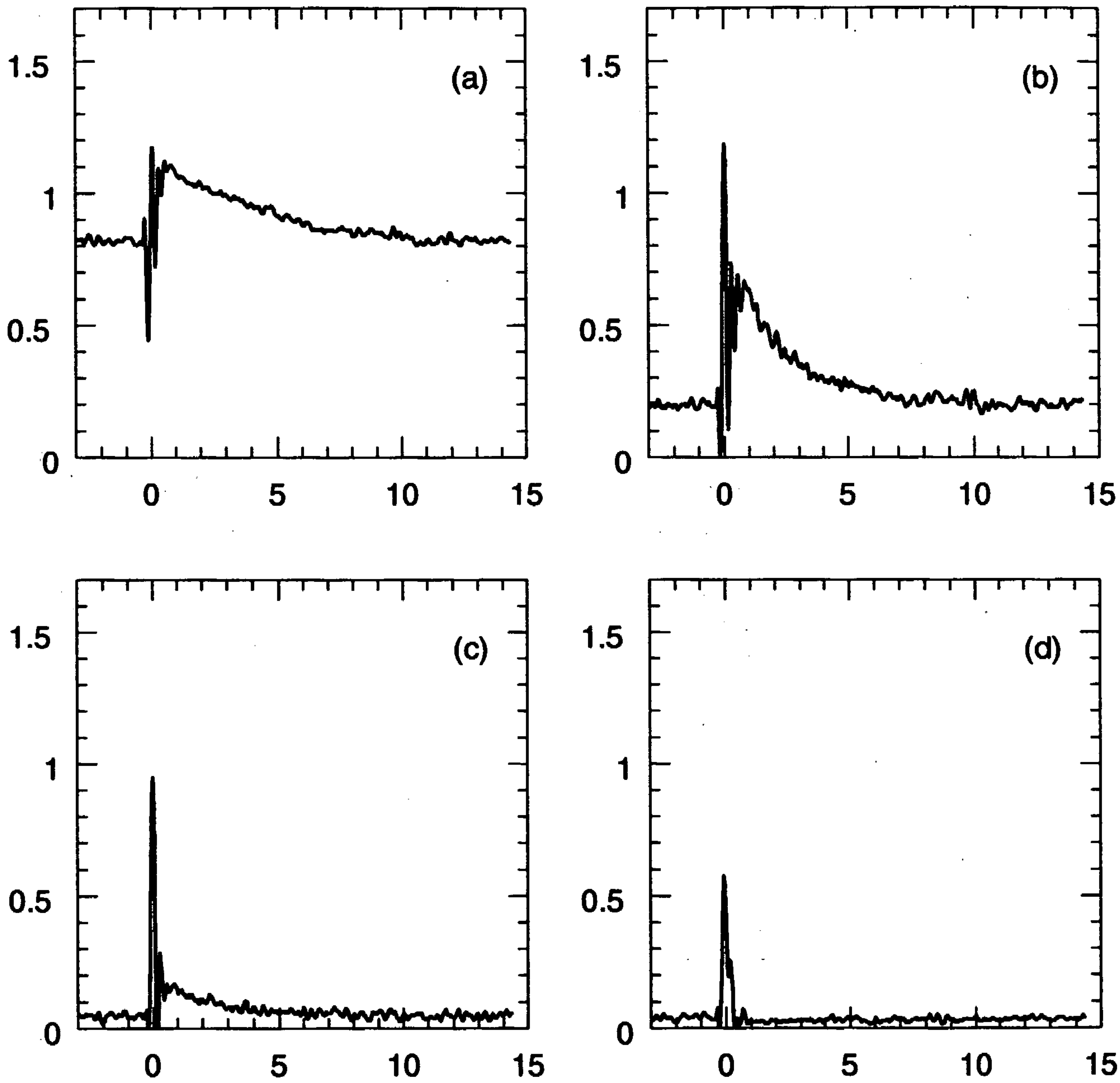
(a)
(b)
(c)
(d)
1.5
1
0.5
0
0
5
10
15

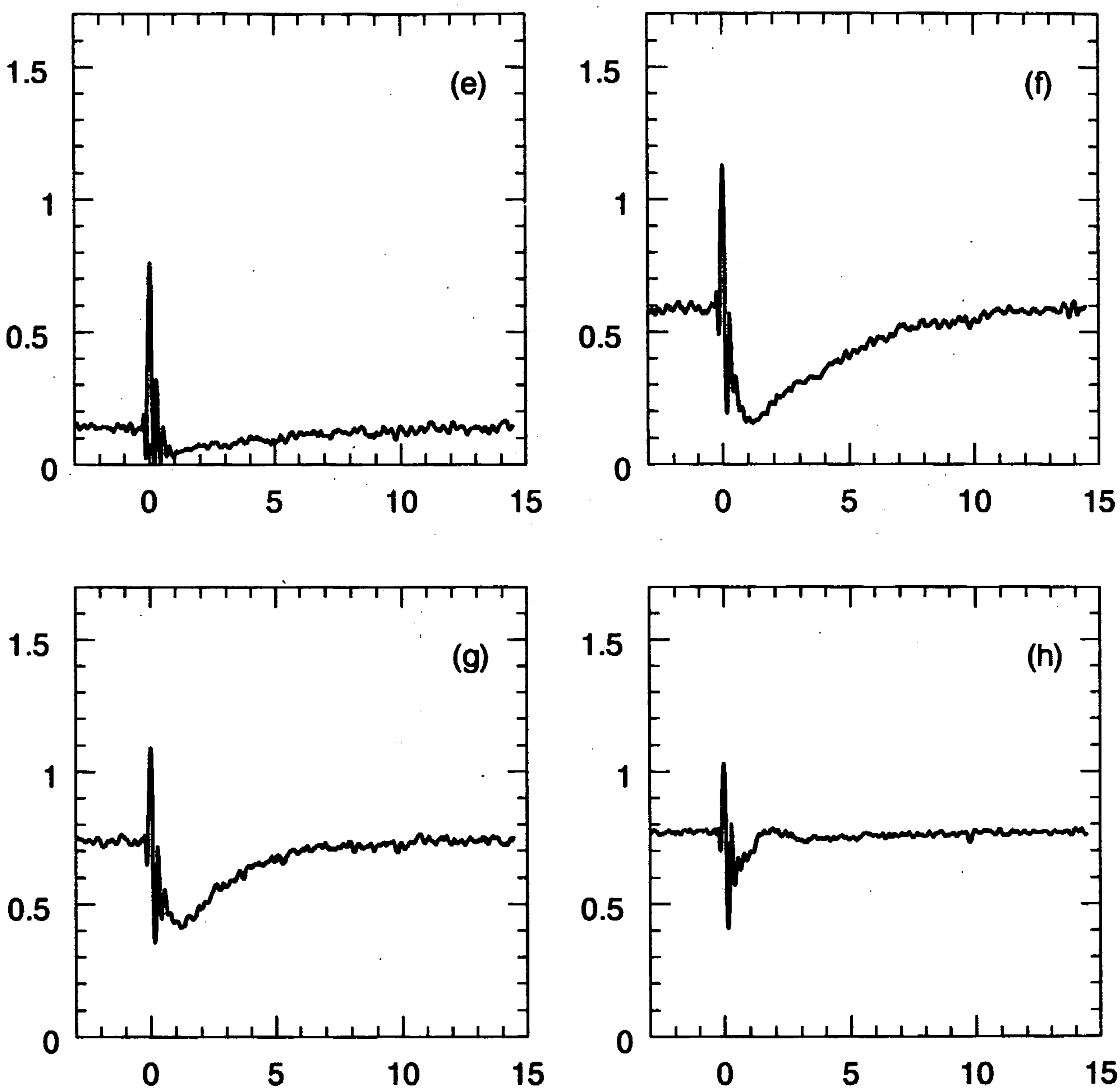

(e)
(f)
(g)
(h)
1.5
1
0.5
0
0
5
10
15

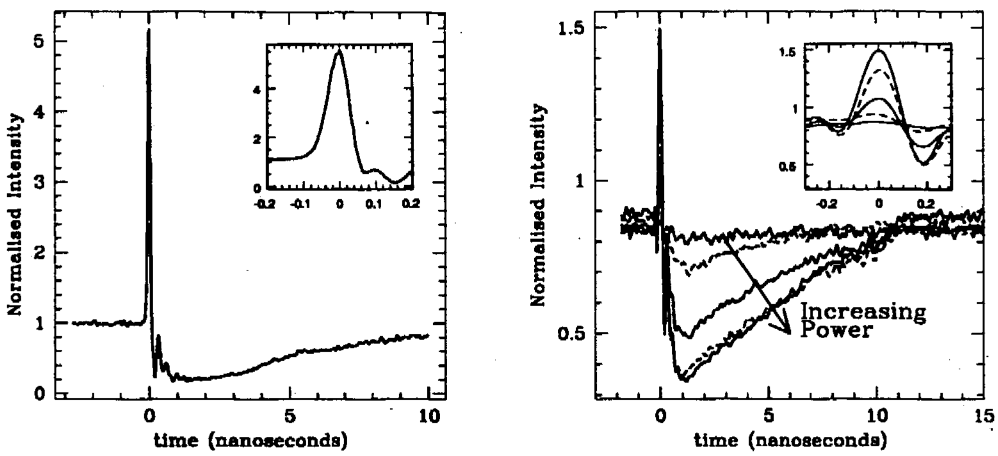
Normalised Intensity
time (nanoseconds)
Normalised Intensity
time (nanoseconds)
Increasing
Power

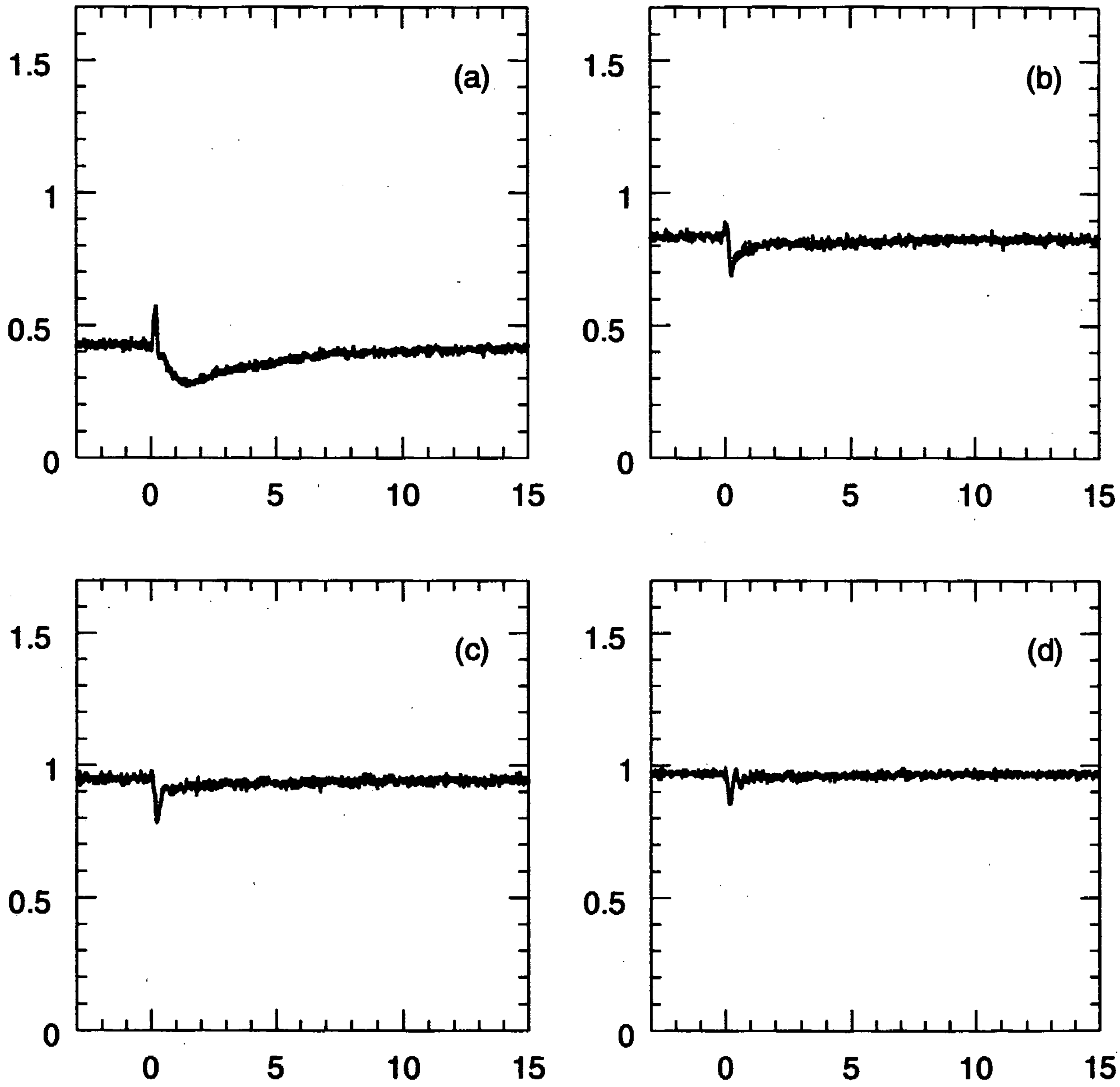

1.5
1
0.5
0
0
5
10
15
(a)
(b)
(c)
(d)

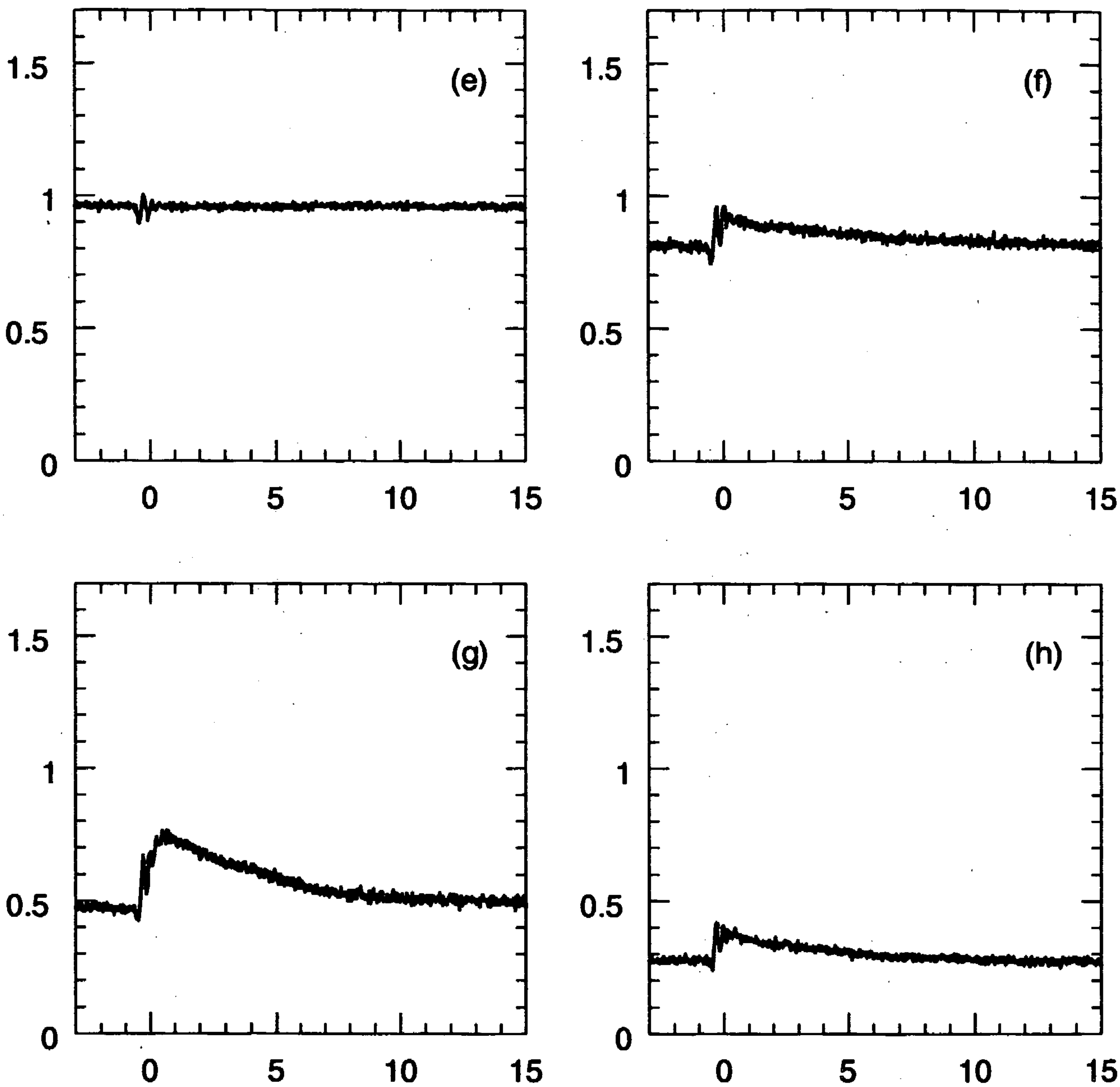

1.5
1
0.5
0
0
5
10
15
(e)
(f)
(g)
(h)